

Nonlinear absorption edge properties of 1.3- μm GaInNAs saturable absorbers

R. Grange,^{a)} A. Rutz, V. Liverini, M. Haiml, S. Schön, and U. Keller

ETH Zurich, Physics Department, Institute of Quantum Electronics, Wolfgang-Pauli-Strasse 16, CH-8093 Zurich, Switzerland

(Received 29 April 2005; accepted 3 August 2005; published online 20 September 2005)

GaInNAs 1.3- μm quantum-well saturable absorber mirrors are characterized with spectrally resolved nonlinear reflectivity measurements over 70 nm around the broadened band edge. All important parameters such as saturation fluence F_{sat} , modulation depth ΔR , and nonsaturable loss ΔR_{ns} are obtained relative to the photoluminescence (PL) peak. F_{sat} has a minimum of $4 \mu\text{J}/\text{cm}^2$ 10 nm above the PL peak and ΔR scales with the linear absorption even in the bandtail. The product $\Delta R \cdot F_{\text{sat}}$ important to suppress Q -switching instabilities in mode-locked lasers decreases linearly with wavelength and reaches a minimum 20 nm above the PL peak. We observed wavelength-independent nonsaturable losses of only about 10% of the maximum linear absorption. These results increase the understanding of optical and electronic properties of GaInNAs around the band edge. © 2005 American Institute of Physics. [DOI: 10.1063/1.2058216]

Solid-state lasers passively mode-locked with semiconductor saturable absorber mirrors^{1,2} (SESAMs) are reliable compact ultrafast sources.³ The choice of the SESAM material is crucial for self-starting and stable operation of the laser at tens of GHz repetition rates.⁴ So far, InGaAsP,⁵ InGaAs,^{6,7} and AlGaAsSb (see Ref. 8) have been demonstrated as absorbers for the wavelength range from 1.3 to 1.5 μm . More recently, dilute nitrides have been used as long-wavelength absorber material. This quaternary alloy has the advantage to be GaAs-based and to minimize the lattice mismatch by incorporating just a few percent of nitrogen to InGaAs while reducing the indium concentration.⁹ We showed that GaInNAs SESAMs have smaller nonsaturable losses than InGaAs SESAMs at 1.3 μm and we demonstrated stable self-starting passive mode locking at 1314 nm.¹⁰ Quasi-cw pumped Nd:YLF (yttrium lithium fluoride) and Nd:YALO (yttrium aluminate) laser at 1.3 μm with GaInNAs SESAMs have been demonstrated earlier.¹¹ Recently we have achieved up to 10 GHz pulse repetition rate at 1342 nm using optimized GaInNAs SESAMs.¹²

Stable passive mode locking of a solid-state laser with a SESAM requires careful adjustment of the SESAM and laser cavity designs.^{13,14} High-pulse-repetition-rate solid-state lasers require saturable absorbers with small saturation fluence F_{sat} and small modulation depth ΔR , typically below 0.5%. Therefore, very accurate nonlinear reflectivity measurements are necessary to target the desired laser parameters.¹⁵ For instance, very precise measurement of ΔR and F_{sat} is necessary to determine the Q -switched mode-locking (QML) threshold, which is proportional to $\Delta R \cdot F_{\text{sat}}$.¹⁶ However, low-modulation GaInNAs SESAM parameters are not easily accessible and the right choice of absorber composition is not straightforward. So far, measurements of the photoluminescence (PL) wavelength were used to locate the absorption edge because simple linear SESAM reflectivity measurements do not reveal the absorption edge due to the extremely low modulation depth. The location of the PL wavelength relative to the target laser wavelength was set according to

empirical experience. The broad PL spectrum of GaInNAs implies also a broad absorption edge and simple empirical guidelines are not sufficient to optimize the GaInNAs device design. Of particular interest is, therefore, the wavelength for the smallest possible saturation fluence and the smallest possible product of $\Delta R \cdot F_{\text{sat}}$ with respect to the PL peak wavelength. Here we publish for the first time a spectrally resolved nonlinear optical characterization around the absorption edge of GaInNAs SESAMs optimized for high-repetition-rate diode-pumped solid-state lasers.

The GaInNAs SESAM was grown by molecular-beam epitaxy (MBE) on a GaAs (100) substrate. It consists of an 11 nm single-quantum-well (SQW) absorber embedded in a 93 nm GaAs spacer layer and a 93 nm GaAs cap grown on top of a 30-pair AlAs/GaAs distributed Bragg reflector (DBR) centered at 1320 nm. The x-ray diffraction (XRD) rocking curve gives an indium concentration of $\sim 34.8\%$ and a nitrogen concentration of $\sim 1.1\%$. The linear reflectivity of the antiresonant SESAM measured with a CARY 5E spectrophotometer is shown in Fig. 1 (dotted line).

For the full characterization we used five different SESAM pieces all based on the same MBE growth run: one as-grown and four SESAMs annealed at temperatures be-

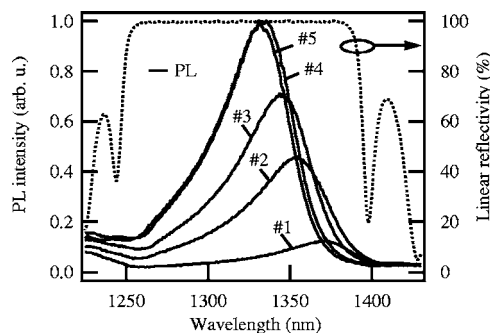


FIG. 1. Photoluminescence intensities (solid lines, arb. u.) and linear reflectivity (dotted line) of the GaInNAs SESAMs vs the wavelength. #1: 1317 nm (as-grown); #2: 1354 nm (1 min RTA at 560 °C); #3: 1345 nm (1 min RTA at 580 °C); #4: 1334 nm (1 min RTA at 600 °C); and #5: 1330 nm (1 min RTA at 600 °C and 1 min at 560 °C).

^{a)}Electronic mail: grange@phys.ethz.ch

tween 560 and 600 °C for 1 or 2 min. In addition, for increased measurement accuracy in the band tail, where the modulation depth becomes very small, we deposited a 220 nm SiO₂ dielectric layer by electron-beam evaporation on top of each of the five different SESAMs just mentioned to increase the field enhancement factor in the absorber by a factor of about 2. We have verified that the coating process does not change the absorber properties: the GaInNAs SESAMs feature broad PL spectra with maxima at 1371 nm to 1330 nm (Fig. 1: solid lines) that are nearly at the same wavelength (± 2 nm) before and after the SiO₂ deposition, contrary to plasma-enhanced chemical vapor deposition of SiO₂ and Si₃N₄.¹⁷ As mentioned earlier, the shape of the absorption spectrum is not revealed from linear reflectivity measurements using a simple spectrophotometer. Thus, we performed nonlinear reflectivity measurements on the SQW SESAMs just described and linear transmission measurements on a multi-quantum-well (MQW) SESAM structure (eleven 10-nm GaInNAs QWs with 60-nm GaAs barriers and fourteen 10-nm GaInNAs QWs with 20-nm GaAs barriers). XRD measurements of both single and MQW structures prove that the well compositions have almost the same indium and nitrogen concentrations of $\sim 35\%$ and $\sim 1.2\%$, respectively.

We used a commercial tunable optical parametric oscillator with 80 MHz repetition rate, 200 fs pulse duration, and 17 nm full width at half-maximum spectral bandwidth. Spectrally resolved measurements were performed from 1330 to 1360 nm in 5-nm increments on each of the 5 SESAMs.¹⁵ The tuning range was limited by the laser source on the short-wavelength range and by the DBR on the long-wavelength range. To enlarge the accessible tuning range, we take advantage of the specific GaInNAs behavior to blueshift the PL spectrum with postgrowth rapid thermal annealing (RTA). Usually this feature is exploited for targeting the right PL wavelength. Here we use it to enlarge the tuning range relative to PL peak wavelength λ_{PL} from 30 nm to about 70 nm. It has been demonstrated that no change in the stoichiometry of the QW occurs upon RTA.¹⁸ We have shown that the decay times do not change significantly upon RTA, and our measurements have demonstrated that the shape of the absorption does not significantly change for moderate RTA temperatures up to 600 °C. Most likely this applies even for higher temperatures. Consequently, the presented data are valid for 1.3 μm GaInNAs in general and not only for a specific annealing temperature.

Figure 2 displays the nonlinear optical parameters (full squares for ΔR , empty squares for $\Delta R + \Delta R_{\text{ns}}$, and crosses for F_{sat}) versus the laser wavelength λ relative to the PL peak λ_{PL} . We concatenate the results obtained with the five SESAMs according to their respective PL peak. The nonsaturable losses ΔR_{ns} of 0.2%, which are only about 10% of the maximum linear absorption, are nearly constant over the whole measurement range and only become comparable or larger than ΔR for $\lambda > \lambda_{\text{PL}} + 30$ nm. The origin of nonsaturable losses could be transmission losses through the DBR, free carrier absorption (FCA), or nonsaturable defect absorption in the absorber. We measured the transmission losses through one SESAM to be almost negligible (less than 0.03%), which confirms the good quality of the DBR. In case of FCA, we would expect ΔR_{ns} to increase for shorter wavelengths where a higher free carrier density is needed to reach transparency, but ΔR_{ns} remains constant. Therefore, nonsat-

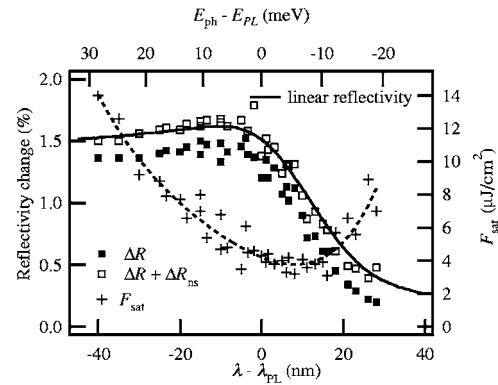


FIG. 2. Nonlinear parameters such as saturation fluence F_{sat} (crosses, right axis), modulation depth ΔR (full squares, left axis), added with the nonsaturable losses $\Delta R + \Delta R_{\text{ns}}$ (empty squares, left axis) of the GaInNAs SQW SESAMs and linear absorption (solid line, arb. u.) of the MQW around the band edge. Bottom axis gives the laser wavelength λ relative to the PL wavelength λ_{PL} . Top axis gives the corresponding photon energies E_{ph} relative to the PL peak E_{PL} .

urable defect absorption is probably the main contribution to ΔR_{ns} .

The linear losses are proportional to $100\% - R_{\text{lin}} = \Delta R + \Delta R_{\text{ns}}$. For comparison, the linear absorption obtained from the transmission measurement of the MQW SESAM annealed at 600 °C for 1 min is plotted in Fig. 2 (solid line) which fits well with $\Delta R + \Delta R_{\text{ns}}$ (open squares) obtained for different annealing temperatures from the five SQW SESAMs. This further supports our conclusion that annealing at moderate temperatures blueshifts mainly the band edge of GaInNAs but does not significantly affect the nonlinear parameters and their spectral dependence.

The saturation fluence (Fig. 2, crosses) has a minimum at $\lambda \approx \lambda_{\text{PL}} + 10$ nm. F_{sat} increases about linearly with decreasing λ for $\lambda < \lambda_{\text{PL}}$ with a slope of $0.35 \mu\text{J}/\text{cm}^2/\text{nm}$ for a field enhancement of 0.76 in the absorber. This linear dependence is due to the constant density of states in a QW and to thermalization: excited carriers fill the bands from their bottom up to the states resonant with the laser wavelength. Obviously, at the band edge F_{sat} will not reach zero, but will have a value determined by the thermal broadening of the Fermi-Dirac distribution, the effective masses of electrons and holes, and the spectral width of the laser pulses. In our case we observe a minimum of $4 \mu\text{J}/\text{cm}^2$ at $\lambda \approx \lambda_{\text{PL}} + 10$ nm, where ΔR is about 60% of its maximum value. In the band tail, F_{sat} increases again for longer wavelengths because of a lower absorption cross section and less overlap between absorber and laser spectrum.

Figure 3 displays the product $\Delta R \cdot F_{\text{sat}}$ versus wavelength. It decreases linearly for $\lambda < \lambda_{\text{PL}}$ with increasing wavelength, which is consistent with the theory described earlier. We observe an even more linear dependence as compared to F_{sat} versus $\lambda - \lambda_{\text{PL}}$ only, as a varying absorption cross section σ_{abs} cancels in the product: ΔR is proportional to σ_{abs} , F_{sat} inversely proportional to σ_{abs} . In the band tail, $\Delta R \cdot F_{\text{sat}}$ slowly decreases down to $20 \text{ nJ}/\text{cm}^2$. Accurate measurements for $\lambda > \lambda_{\text{PL}} + 30$ nm are challenging because ΔR becomes very small and F_{sat} rather high. However, even if $\Delta R \cdot F_{\text{sat}}$ might become a little bit smaller, the individual values of ΔR and F_{sat} do not fit most devices' needs any more for such a large λ_{PL} offset. Note that $\Delta R \cdot F_{\text{sat}}$ is the maximum fluence that gets absorbed by the (saturable) band-to-band transition.¹⁹ Accordingly, $\Delta R \cdot F_{\text{sat}} / \hbar \omega$ is the maximum

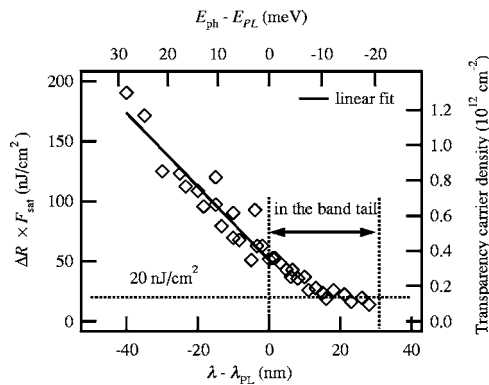


FIG. 3. Product of the saturation fluence and the modulation depth $\Delta R \cdot F_{\text{sat}}$ around the band edge versus the relative wavelength offset $\lambda - \lambda_{\text{PL}}$. Right axis: corresponding transparency carrier density $\Delta R \cdot F_{\text{sat}} / \hbar \omega$.

amount of absorbed photons, which is equal to the transparency carrier density of the absorber plotted on the right axis of Fig. 3. Finally, 1.3- μm GaInNAs SESAMs with low saturation fluences and low QML thresholds are obtained when the PL peak is 10 to 30 nm shorter than the laser wavelength. This can be easily adjusted by postgrowth annealing, as the nonlinear optical properties do not change significantly upon moderate annealing.

In conclusion, we presented the first detailed spectrally resolved characterization of nonlinear optical properties of saturable absorbers. This is especially useful for SQW GaInNAs SESAMs around the broad absorption edge because the behavior in the band tail was not *a priori* predictable. The spectrally resolved measurement gives a concrete design guideline to optimize the GaInNAs SESAMs with simple PL measurement to locate the absorption edge and predict its nonlinear optical parameters around the absorption edge. We observed that the maximum of the PL emission wavelength λ_{PL} corresponds to the maximum of the absorption measurements. The saturation fluence has a minimum where the modulation depth dropped to 60% of the peak value, which occurs at $\lambda_{\text{PL}} + 10$ nm. The smallest values of $\Delta R \cdot F_{\text{sat}}$ required to suppress Q-switching instabilities are observed around $\lambda_{\text{PL}} + 20$ nm. For longer wavelengths F_{sat} becomes too high and ΔR too low for most applications. With the data presented, the efforts to optimize SESAM designs for specific laser oscillators are strongly reduced. The epitaxy requirements are also reduced because the target

PL wavelength can easily be reached with postgrowth RTA processing.

The authors would like to thank H. Rusterholz for the growth of the Bragg mirrors. This work was supported by the Quantum Photonics National Centre of Competence in Research, (QP-NCCR) Switzerland and the KTI project 5781.1 KTS.

- ¹U. Keller, D. A. B. Miller, G. D. Boyd, T. H. Chiu, J. F. Ferguson, and M. T. Asom, *Opt. Lett.* **17**, 505 (1992).
- ²U. Keller, K. J. Weingarten, F. X. Kärtner, D. Kopf, B. Braun, I. D. Jung, R. Fluck, C. Hönninger, N. Matuschek, and J. Aus der Au, *IEEE J. Sel. Top. Quantum Electron.* **2**, 435 (1996).
- ³U. Keller, *Nature (London)* **424**, 831 (2003).
- ⁴R. Paschotta, L. Krainer, S. Lecomte, G. J. Spühler, S. C. Zeller, A. Aschwanen, D. Lorenser, H. J. Unold, K. J. Weingarten, and U. Keller, *New J. Phys.* **6**, 174 (2004).
- ⁵R. Fluck, R. Häring, R. Paschotta, E. Gini, H. Melchior, and U. Keller, *Appl. Phys. Lett.* **72**, 3273 (1998).
- ⁶R. Fluck, G. Zhang, U. Keller, K. J. Weingarten, and M. Moser, *Opt. Lett.* **21**, 1378 (1996).
- ⁷S. C. Zeller, L. Krainer, G. J. Spühler, R. Paschotta, M. Golling, D. Ebling, K. J. Weingarten, and U. Keller, *Electron. Lett.* **40**, 875 (2004).
- ⁸R. Grange, O. Ostinelli, M. Haiml, L. Krainer, G. J. Spühler, S. Schön, M. Ebnöther, E. Gini, and U. Keller, *Electron. Lett.* **40**, 1414 (2004).
- ⁹M. Kondow, T. Kitatani, S. Nakatsuka, M. C. Larson, K. Nakahara, Y. Yazawa, M. Okai, and K. Uomi, *IEEE J. Sel. Top. Quantum Electron.* **3**, 719 (1997).
- ¹⁰V. Liverini, S. Schön, R. Grange, M. Haiml, S. C. Zeller, and U. Keller, *Appl. Phys. Lett.* **84**, 4002 (2004).
- ¹¹H. D. Sun, G. J. Valentine, R. Macaluso, S. Calvez, D. Burns, M. D. Dawson, T. Jouhti, and M. Pessa, *Opt. Lett.* **27**, 2124 (2002).
- ¹²G. J. Spühler, L. Krainer, V. Liverini, S. Schön, R. Grange, M. Haiml, A. Schlatter, S. Pawlik, B. Schmidt, and U. Keller, *IEEE Photonics Technol. Lett.* **17**, 1319 (2005).
- ¹³U. Keller, in *Nonlinear Optics in Semiconductors*, edited by E. Garmire and A. Kost (Academic, Boston, 1999), Vol. 59, pp. 211.
- ¹⁴U. Keller, *Prog. Opt.* **46**, 1 (2004).
- ¹⁵M. Haiml, R. Grange, and U. Keller, *Appl. Phys. B: Lasers Opt.* **79**, 331 (2004).
- ¹⁶C. Hönninger, R. Paschotta, F. Morier-Genoud, M. Moser, and U. Keller, *J. Opt. Soc. Am. B* **16**, 46 (1999).
- ¹⁷H. F. Liu, C. S. Peng, E.-M. Pavelescu, T. Jouhti, S. Karirinne, J. Kontinen, and M. Pessa, *Appl. Phys. Lett.* **84**, 478 (2004).
- ¹⁸P. J. Klar, H. Grüning, J. Koch, S. Schäfer, K. Volz, W. Heimbrodt, A. M. Kamal Saadi, A. Lindsay, and E. P. O'Reilly, *Phys. Rev. B* **64**, 121203 (2001).
- ¹⁹R. Paschotta, J. Aus der Au, G. J. Spühler, F. Morier-Genoud, R. Hövel, M. Moser, S. Erhard, M. Karszewski, A. Giesen, and U. Keller, *Appl. Phys. B: Lasers Opt.* **70**, S25 (2000).